Electronic Supplementary Material (ESI) for Journal of Materials Chemistry C.

Supporting Information

An Integrated Self-Healable and Robust Conductive Hydrogel for Dynamically Self-Adhesive and Mechanically Conformable E-Skin

Changyou Shao, Lei Meng, Chen Cui, Jun Yang*

Beijing Key Laboratory of Lignocellulosic Chemistry, Beijing Forestry University, No 35, Tsinghua East Road, Haidian District, Beijing, 100083, China

Experimental Section

Materials. The never-dried bleached softwood Kraft pulp fibers was provided by DongHua Pulp Factory, China. Tannic acid (TA), acrylic acid (AA), Aniline (ANI, 99.5%), ammonium persulfate (APS), N,N′-methylenediacrylamide (MBA), hydrochloric acid (37.5 wt%), Tris(hydroxymethyl)-aminomethane (Tris) were purchased from Beijing Lanyi Co. Ltd., China. The photoinitiator, Irgacure 2959 (2-hydroxy-1-[4-(2-hydroxyethoxy)phenyl]-2-methyl-1-propanone) was purchased from Sigma-Aldrich. All other chemicals were analytical grade unless otherwise noted andwere used as received.

Extraction of Cellulose Nanocrystals. Cellulose nanocrystals (CNCs) were prepared by the well-established sulfuric acid hydrolysis method with minor modifications.[1] In detail, 4 g of pulp fibers were cut into small pieces and then added into 200 mL of 60 wt% sulfuric acid at 50 °C for 2 h under mechanical stirring (350 rpm), where amorphous regions were preferentially hydrolyzed. The suspension was diluted with deionized water and concentrated by centrifugation, followed by dialysis against water until pH neutrality. Finally, high-pressure homogenization was applied to increase dispersity and stability of the suspension, the homogenized CNC suspension (∼1.02 wt %) was cryopreserved (4 °C) before usage.

Preparation of Tannic Acid Coated Cellulose Nanocrystals (TA@CNC). The TA@CNC suspension was prepared via a one-pot water-based process. Briefly, Tris buffer solution (1 M) was dropwise added into the 150 g CNC suspension (~1.02 wt %, containing about 1.53 g CNCs) until pH was adjusted to 8.0. Subsequently, 0.51 g of tannic acid (TA) was introduced and the resultant suspension was magnetically stirred for 6 h at room temperature, obtaining the final TA@CNC suspension with concentration of 1.2 wt % in this work.

Hydrogels Preparation. The robust and conductive TC-Gel was prepared by in suit synthesizing polyaniline in the poly(acrylic acid) hydrogels reinforced by the TA@CNC. Initially, 5 g of AA monomer, 15 mg of UV initiator, and 20 mg of MBA chemical cross-linker were dissolved in 11 mL of deionized water. Then 4 g TA@CNC aqueous suspension (~1%) was added and stirred vigorously for 10 min, followed by sonication in an ice-water bath for 10 min to form a uniform mixture. After degassing by bubbling nitrogen for 5 min, the mixture was poured into PTFE molds under nitrogen atmosphere at 50 °C for 2 h to achieve the covalently cross-linked composite gels, coded as T-Gel. Afterward, the as-prepared T-Gel was immersed into sufficient aniline/hydrochloric acid (molar ratio of 1:5) aqueous solution, which was placed in an ice/water bath. Then, APS with the dose consistent with aniline was added into the precursor solution to trigger the polymerization of aniline. Finally, the TC-Gel was obtained after aniline completely polymerized for 6 h, and washed with deionized water for several times. The obtained TC-Gel was stored at 4 °C for further characterization.

As control, the pure poly(acrylic acid) hydrogels (PAA) and conductive hydrogel (C-Gel) by in-situ synthesized aniline in pure PAA hydrogels were also prepared according to the same method.

Characterization. For cross-section observation by scanning electronmicroscopy (SEM, Hitachi 3500S), the fractured hydrogel samples were freeze-dried for 48 h, followed by putter-coating with platinum for 30 s observation at an accelerating voltage of 6 kV. Attenuated total reflectance-Fourier transform infrared spectroscopy (ATR-FTIR) examinations were conducted on a Nicolet 6700 (Thermo Scientific, USA) from 650 and 4000 cm^{-1}.

Mechanical Tests. All mechanical tests were performed at room temperature using a universal mechanical tester (Zwell/Roell) equipped with a 200 N load cell. The uniaxial tensile test was performedon the rectangular-shape specimens (10 mm in width, 2 mm in depth,and 80 mm in length). The initial distance between two clamps was 15mm, and the constant stretching rate was 100 mm/min. The unconfined compression tests of the cylindrical sample (30 mm height and 20 mm diameter) were conducted at a crosshead speed of 10 mm/min. Self-recovery properties were investigated by cyclic tensile and compressive loading-unloading tests with the same specimens at equal test speeds. Toughness (*T*) was estimated by the area under the stress-strain curves until fracture point by following equation:

$$T = \int_{\varepsilon_0}^{\varepsilon_f} \sigma(\varepsilon) d\varepsilon$$

where ε_0 and ε_f corresponded to the initial stretch and fracture strain, respectively.

Peeling Measurement. To assess the peeling adhesive strength, the standard 90° peeling test was employed for hydrogels adhering to various solid surfaces. The hydrogel samples were prepared with length of 80 mm, width of 10 mm and thickness of 5 mm. First, the hydrogel samples were attached with a stiff backing (cloth foil) in order to prevent its elongation along the peeling direction, keeping original peeling adhesive strength. Then the hydrogel specimen was attached to the surface of solid materials, such as human skin, plastic, rubber, glass, copper, polytetrafluoroethylene (PTFE), bone, and wood for 30 min. Subsequently, the peeling adhesion test was carried out at a rate of 10 mm min^{-1}.

Self-Healing Experiments. The rectangular-shape specimens (10mm in width, 2 mm in depth, and 80 mm in length) were cut into halves using blades, and then the two separate halves were brought into contact immediately without applied stress and were stored in a sealed vessel to minimize the water evaporation. After self-healing, the uniaxial tensile test was measured again to calculate the healing efficiency (HE) (defined as the toughness ratio between the healed gel and original gel).

Electrical Tests. The real-time electrical signals of the strain sensors based on the resistance changes of the hydrogels in a different state were recorded by an electrochemical working station (Autolab 302N, Switzerland) under a constant voltage of 1 V, the corresponding strain was recorded by the universal testing machine.

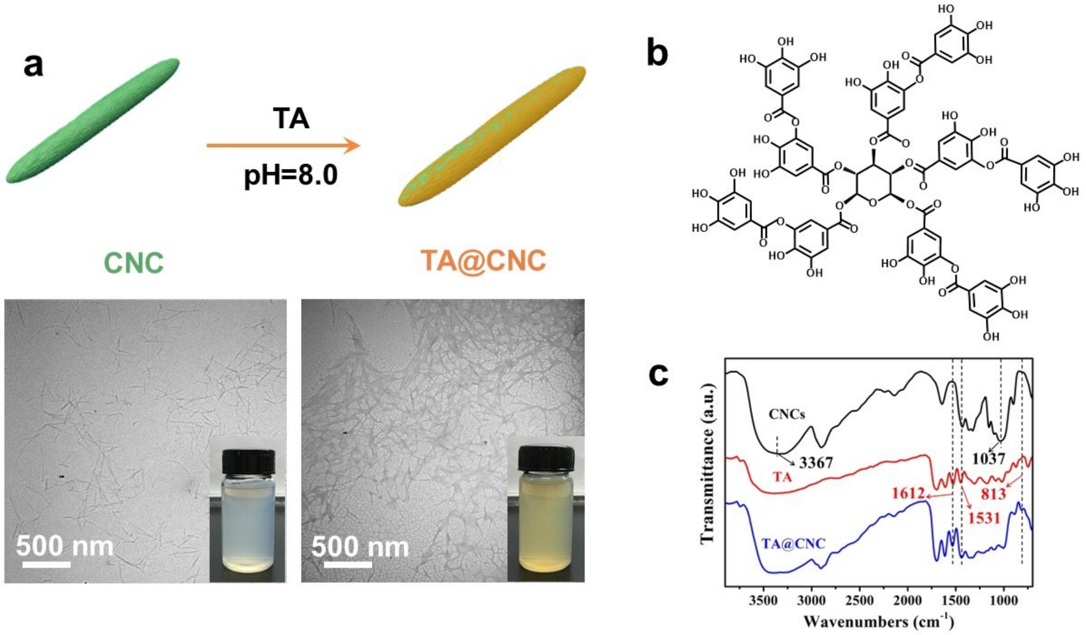

Figure S1. (a) Schematic illustration showing the preparation process of TA@CNC by the surface modification CNC particles, and their corresponding TEM images. (b) Chemical structure of TA. (c) FTIR spectra of CNCs, TA and TA@CNC.

FTIR was used to corroborate the successful surface modification (Figure S1c), where thespectrum of TA@CNC appeared some notable stretching peaks in contrast to native CNCs including a peak at 813cm^{-1} from distortion vibrations of C=C in the benzene ringsand peaks at 1531 and 1612 cm^{-1} from stretching vibrations of the C−C aromatic groups.[2]

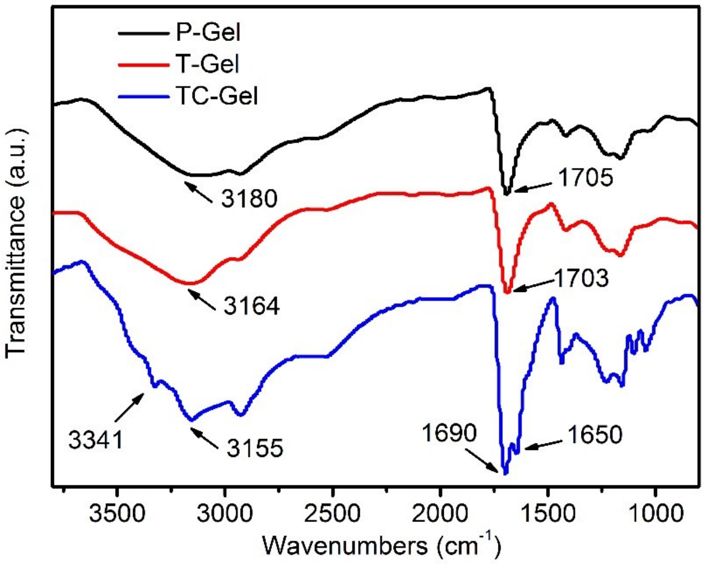

Figure S2. The FT-IR spectra of P-Gel, T-Gel and TC-Gel.

The presence of absorption peak at 3341 cm^{-1} is attributed to the stretching vibration of N-H stretching, implying the existence of PANI in TC-Gel. Besides, it was worth to note that the peak at 3180 cm^{-1} for P-Gel attributed to -OH was shifted to 3164 cm^{-1} for T-Gel and 3155 cm^{-1} for TC-Gel, respectively. The results indicated that more strong hydrogen bonding were formed in T-Gel and TC-Gel due to the introduction of TA@CNC and PANI in hydrogels.[3] The absorption peaks at 1705 and 1703 cm^{-1} are attributed to the stretching band of carbonyl (C=O) for P-Gel and T-Gel, respectively. While in the spectrum of TC-Gel, we observe that the stretching band of carbonyl (C=O) shift to 1690 cm^{-1} , which indicates that carboxyl groups dangled on PAA chains interacte with PANI by electrostatic interactions and thus induced a weak band shift.[4]

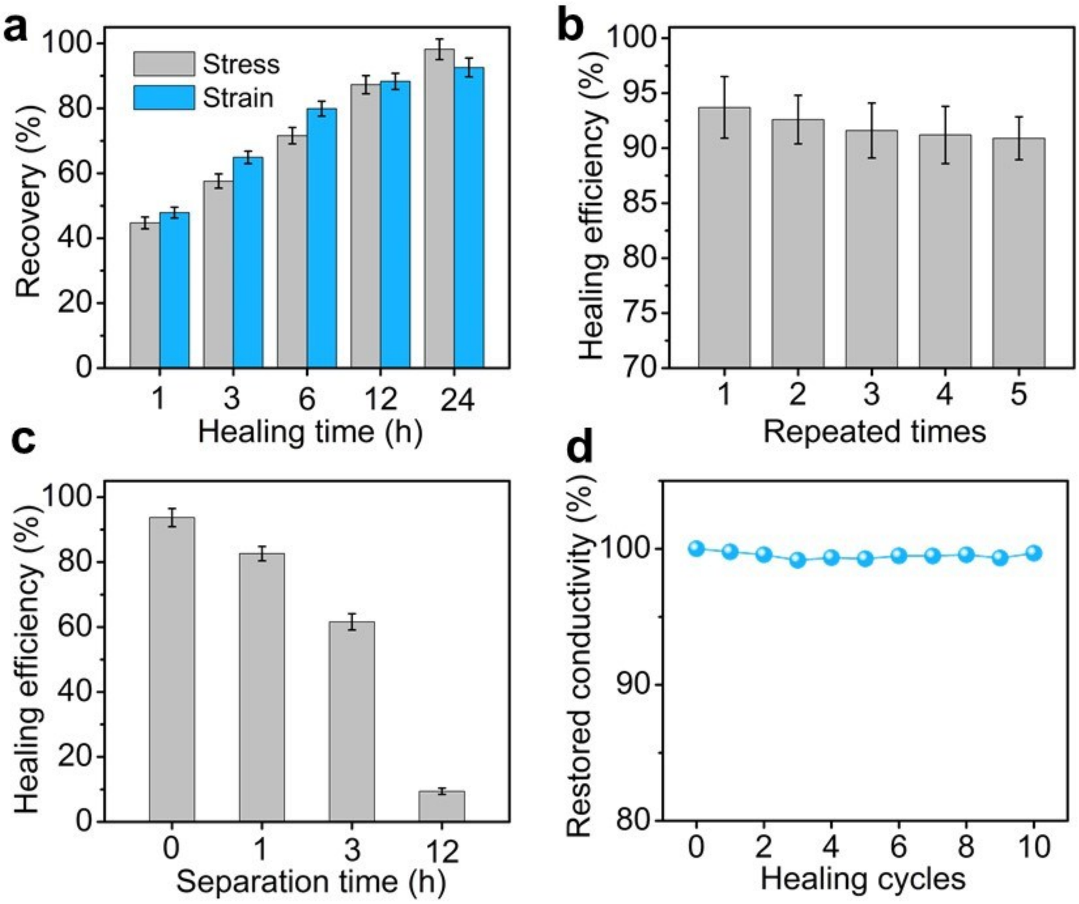

Figure S3. (a) The effect of healing time on the fracture stress and strain of the hydrogel after autonomous self-healing, respectively. (b) The effects of repeated times on healing efficiency of the TC-Gel, healing time is 24 h for each cycle. (c) The effects of separation time on healing efficiency of the TC-Gel after autonomous healing 24 h. (d) Restored conductivity of TC-Gel as function of healing cycles.

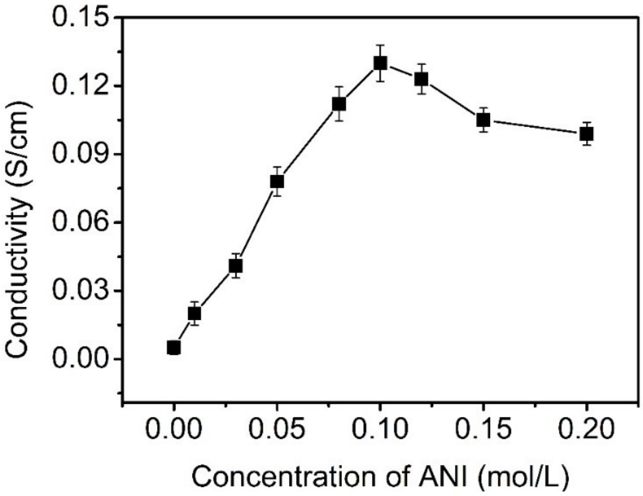

Figure S4. Conductivity of the TC-Gel with different concentration of aniline.

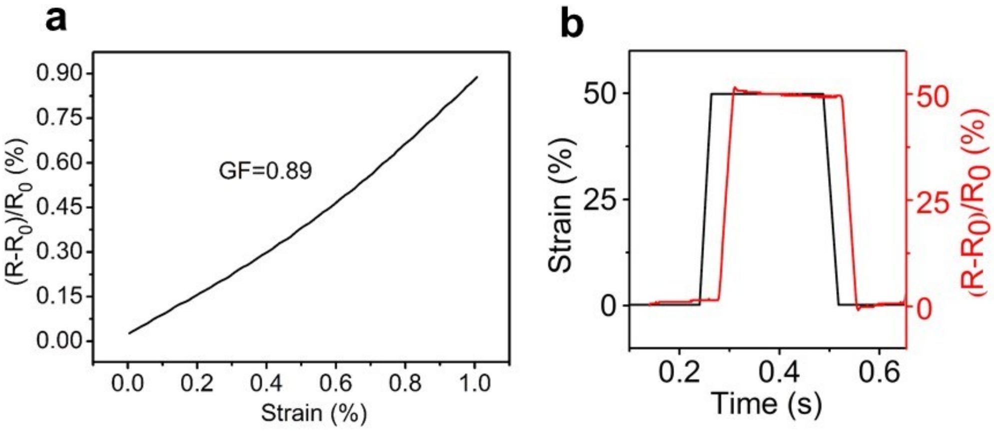

Figure S5. (a) Relative resistance change of TC-Gel sensor within strain range of 0-1%. (b) A magnified view of the relative resistance changes for cycling between 0 and 50% strain

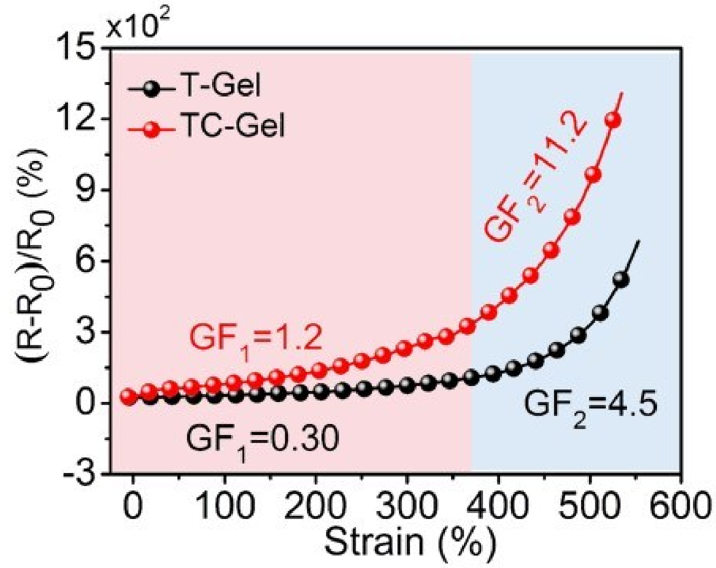

Figure S6. Relative resistance change versus strain for T-Gel and TC-Gel sensor.

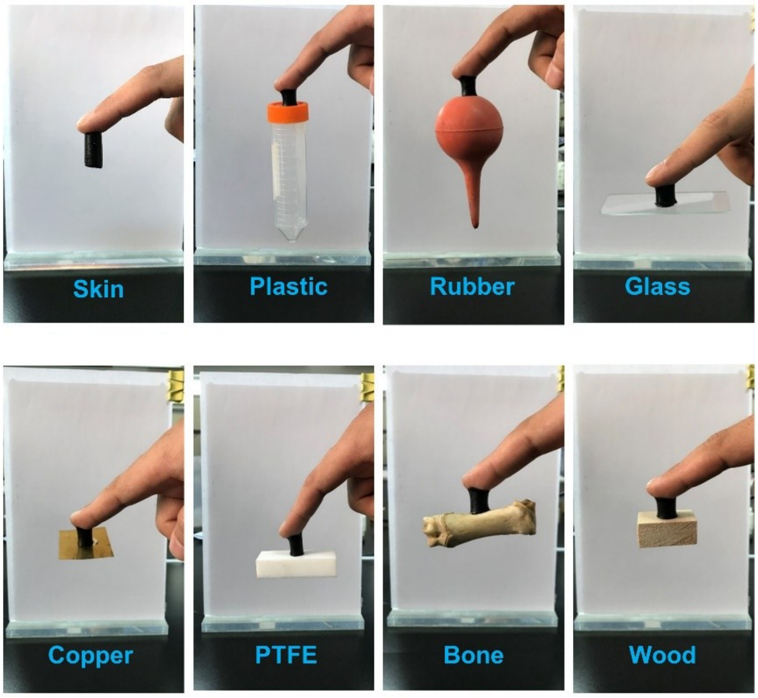

Figure S7. The TC-Gel showing strong adhesion with various surfaces.

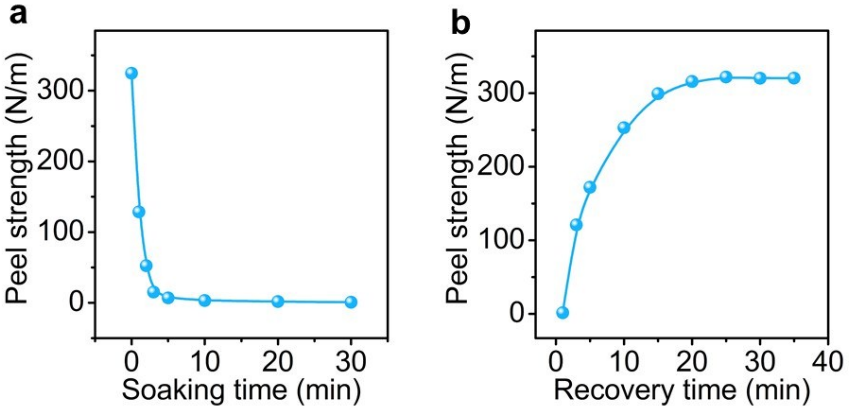

Figure S8. (a) Changes in the peel strength of the TC-Gel as a function of soaking time and (b) recovered peel strength with recovery time.

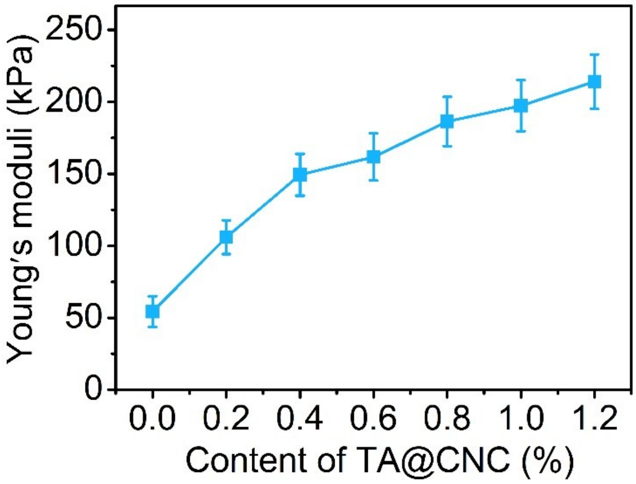

Figure S9. Young's modulus of TC-Gel as a function of content of TA@CNC.

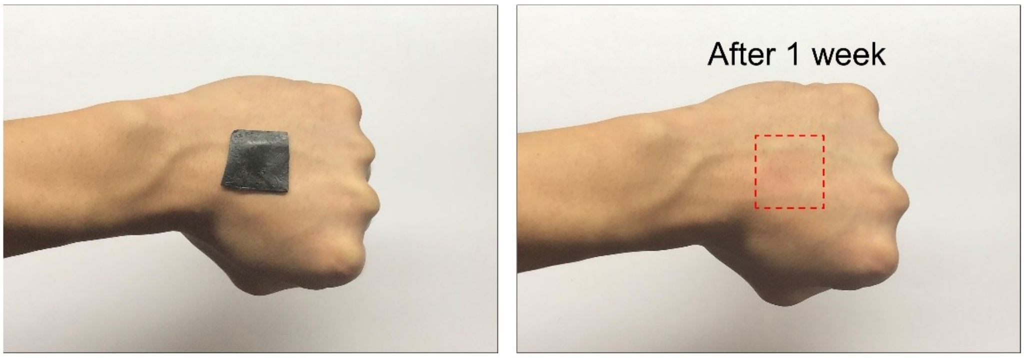

Figure S10. TC-Gel can adhere to human skin for 1 week without any allergy, irritation, and pain and detach without residual.

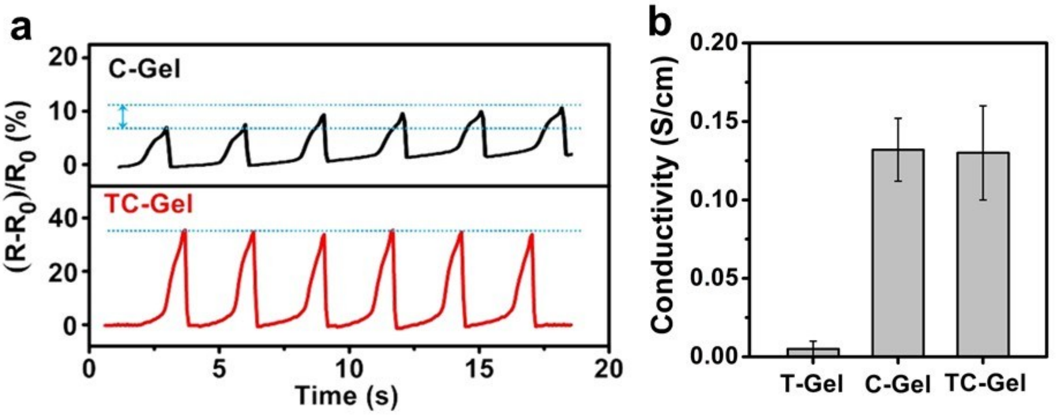

Figure S11. (a) Comparison of TC-Gel and C-Gel assembled sensor in electrical deviation under of 40% strain. (b) Conductivity of T-Gel, C-Gel and TC-Gel.

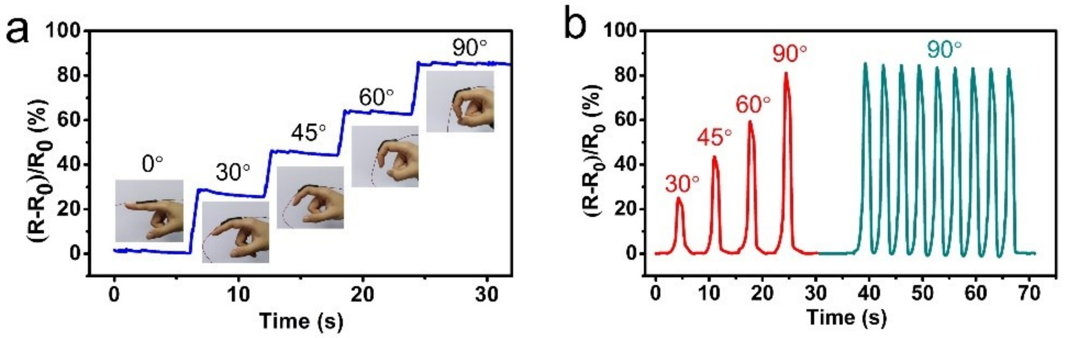

Figure S12. (a) Relative resistance responses of the TC-Gel sensor during the detection of finger bending. The insets show photographs of a TC-Gel sensor directly adheres to the joint of an index finger and finger motions with different finger-bending degrees. (b) Representative resistance signal of the TC-Gel sensor during the bending and unbending of the index finger to angles of 30°, 45°, 60°, and 90°. (b) Relative current responses of the TC-Gel sensor to repeated bending cycles of 90°.

Figure S12 showed that finger bending could be precisely tracked by directly adhering sensor to the joint of an index finger. When the extended finger bent to a certain angle, the relative resistance change of the sensor increased to a certain value and then remained stable. Further bending led to further increase of the relative resistance change, forming a series of stepwise increased signal (Figure S12a). During quick bending-relaxation cycle modes of the finger bent to different angles of 30°, 45°, 60°, and 90°, the relative resistance of the TC-Gel sensor increased with increased bending degree and immediately recovered, while it changed consistently for repeated bending cycles of 90° (Figure S12b), revealing the fast response and stable sensing performance of the TC-Gel sensor.

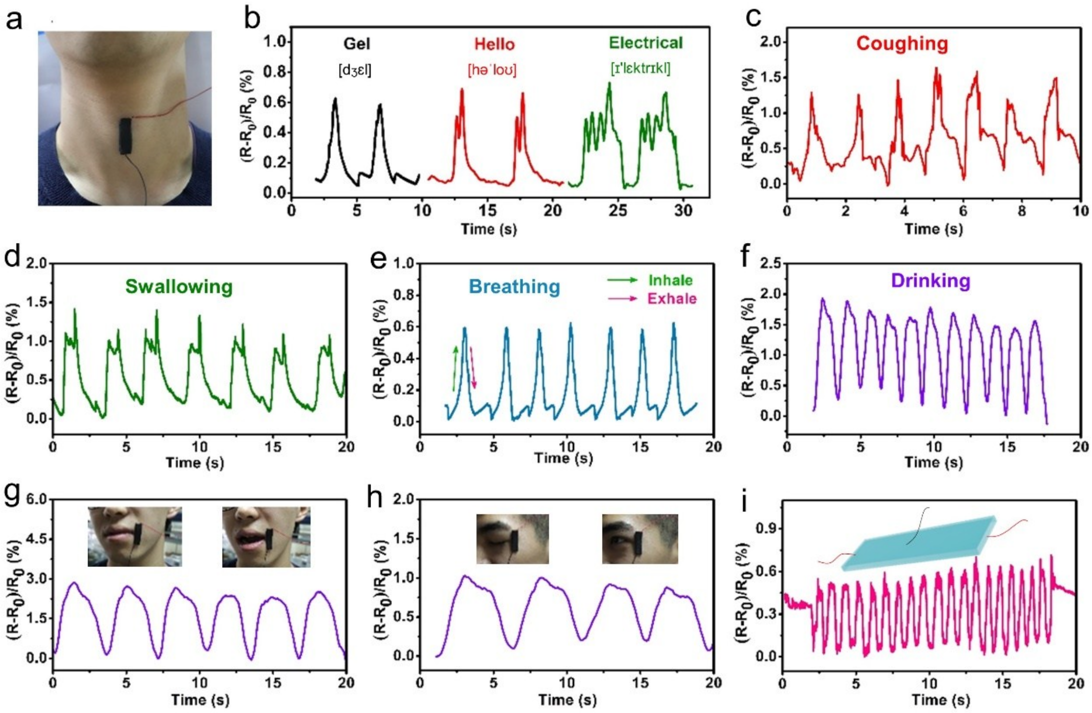

Figure S13. (a) TC-Gel sensor located at the throat for monitoring resistance change versus time during (b) phonation when the wearer spoke “Gel”, “Hello”, and “Electrical”, (c) coughing, (d) swallowing, (e) breathing, and (f) drinking, respectively. Signals showing the tiny muscle movement caused by opening-closing cycles of mouth (g) and eyes (h), the insets show photographs of TC-Gel sensors directly attached to corners of mouth and eye, respectively.

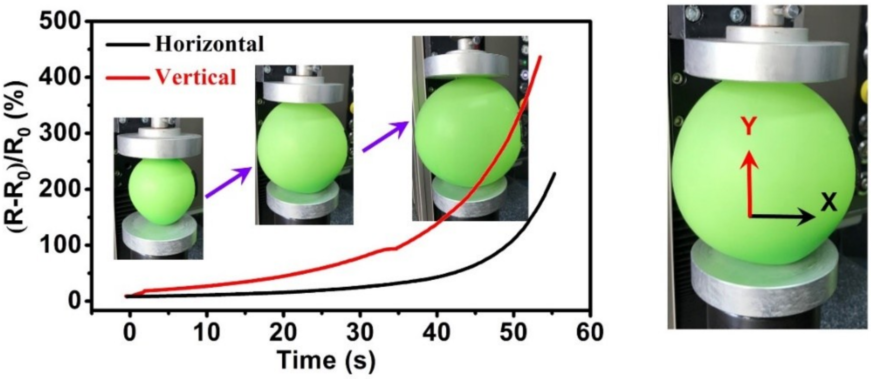

Figure S14. The resistance changes of TC-Gel sensor attached to an air inflating balloon at horizontal and vertical direction, respectively.

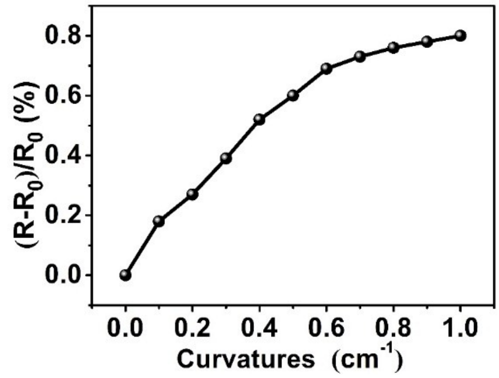

Figure S15. The relatively resistance changes of TC-Gel sensor attached to an air inflating balloon as a function of curvature.

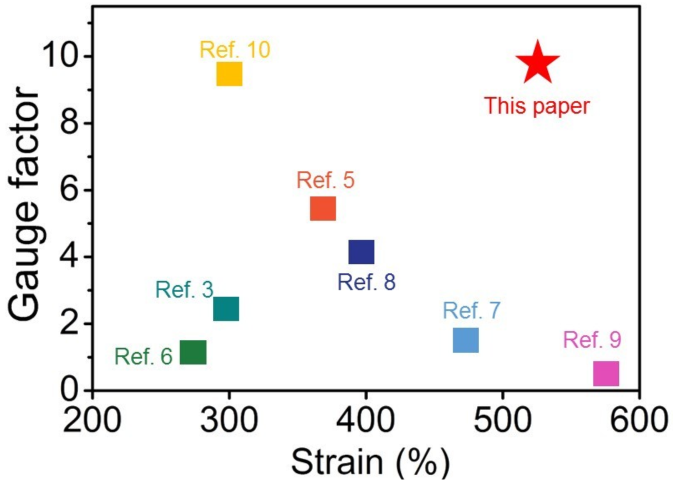

Figure S16. Summary of relationship between gauge factor and strain of reported conductive gel-based strain sensors.[3, 5-10]

References

1. J. Yang, J.-J. Zhao, F. Xu and R.-C. Sun, *ACS Appl. Mater. Interfaces*, 2013, **5**, 12960-12967.
2. S. Kim, T. Gim and S. M. Kang, *ACS Appl. Mater. Interfaces*, 2015, **7**, 6412-6416.
3. Z. Wang, J. Chen, Y. Cong, H. Zhang, T. Xu, L. Nie and J. Fu, *Chem. Mater.*, 2018, **30**, 8062-8069.
4. L. Sun, H. Liu, R. Clark and S. C. Yang, *Synth. Met.*, 1997, **84**, 67-68.
5. J. T. Muth, D. M. Vogt, R. L. Truby, Y. Mengüç, D. B. Kolesky, R. J. Wood and J. A. Lewis, *Adv. Mater.*, 2014, **26**, 6307-6312.
6. L. Wang, G. Gao, Y. Zhou, T. Xu and J. Fu, *ACS Appl. Mater. Interfaces*, 2018, **11**, 3506-3515.
7. Y. Zhou, C. Wan, Y. Yang, H. Yang, S. Wang, Z. Dai, K. Ji, H. Jiang, X. Chen and Y. Long, *Adv. Func. Mater.*, 2019, **29**, 1806220.
8. W. Tao, Z. Ying, Q. Liu, C. Wen and H. Xu, *Adv. Func. Mater.*, 2017, **28**, 1705551.
9. S. Liu and L. Li, *ACS Appl. Mater. Interfaces*, 2017, **9**, 26429-26437.
10. S. Gong, D. T. Lai, B. Su, K. J. Si, Z. Ma, L. W. Yap, P. Guo and W. Cheng, *Adv. Electron. Mater.*, 2015, **1**, 1400063.